Advanced in Engineering and Intelligence Systems

Journal Web Page: https://aeis.bilijipub.com

# Novel Optimization Algorithms Usage to Model the Compressive Strength of Ultra-High-Performance Concrete in Machine Learning Technique: Support Vector Regression

Tianhua Zhou[1,*] , Dorota Mozyrska[2]

[1] *School of Civil Engineering, Chang'an University, Xi'an, Shaanxi, 710061, China*
[2] *Faculty of Computer Science, Bialystok University of Technology, Wiejska 45A, 15-531, Bialystok, Poland*

## Highlights

- Simulating compressive strength of Ultra-High-Performance Concrete using eco-friendly constituents.
- Support Vector Regression combined with Marine Predator Algorithm and Grasshopper Optimization Algorithm utilized for accurate CS simulation.
- Eight components mixed to generate CS and model them, with R2 values of 90% (SVR-MPA) and 89.77% (SVR-GOA).
- RMSE values of 9.41 MPa (SVR-MPA) and 9.98 MPa (SVR-GOA) obtained for error rate assessment.

**Article Info**

Received: 19 February 2023
Received in revised: 23 May 2023
Accepted: 23 May 2023
Available online: 28 June 2023

**Keywords**

Ultra-High-Performance;
Concrete;
Grasshopper
Optimization Algorithm;
UHPC;
Compressive Strength;
Support vector regression;
Marine Predator Algorithm.

**Abstract**

Ultra-High-Performance Concrete (UHPC) is a resistant ingredient in projects requiring analysis of its composition to appraise the UHPC Compressive Strength (CS). Experimentally, assigning the relations between ingredients may require more time, energy, and cost. The intelligent techniques evaluate the compressive strength based on the UHPC composition's ingredients. Selecting environmentally-friendly concrete materials seems one of the prevalent methods used worldwide. This study suggested a machine learning method for predicting the CS of UHPC including support vector regression (SVR). In addition, two meta-heuristic algorithms have been used for improving the accuracy of predicting CS containing the Marine Predator Algorithm (MPA) and Grasshopper Optimization Algorithm (GOA). In this regard, the experimental samples' result has been employed for validating the prediction from published papers. Furthermore, various metrics were used to assess the hybrid modeling performance. As a result, the $R^2$ indicator to model the CS value in the calibration stage for SVR-MPA was obtained at 90 % while for SVR-GOA it was 89.77 %, with a 0.33% difference. Further, for the *RMSE* index, the SVR-MPA could get an error rate of 9.41 MPa, but for SVR-GOA, it was calculated at 9.98 MPa. The comprehensive OBJ index was calculated for SVR-GOA 7.43 as an error that is 15.06 % higher than SVR-MPA, showing the capability of SVR-MPA to overcome errors rather than SVR-GOA.

## 1. Introduction

The concrete type called Ultra-High-Performance (UHPC) is developed for many projects that show excellent properties from the compressive behavior viewpoint, tensile behavior, and durability compared to typical concrete and high-performance concrete (HPC). The research programs to feature a lot of actions related to the use of UHPC in the highway bridge industry have been done [1]. UHPC, as a great achievement composition, gives us acceptable resistance against compressions up to 150 Mega Pascal (MPa) and excellent resistance in any harsh environment. This material is utilized for various mechanisms in diverse structures [2]–[5]. By cutting the cement and micro-silica, the costs and emission of CO2 are reduced, as well as the useful longer service life and properties in comparison with typical or high-strength

* Corresponding Author: Tianhua Zhou
Email: zhoutianhua@chd.edu.cn

concrete defined the high short-term cost and positive effects on the environment. Regarding this matter, due to the cement decline seems to have a key role. It enhances the construction industry's sustainability as an environmental efficiency building [6].

A few investigations have explored the behavior of UHPC and its utilization over a long time [7]. The compressive strength of UHPC ordinarily appears to be between 150 and 810 MPa [8]–[10]. Added substances such as fly ash, nano silicate, metakaolin, and micro-silica have drawn researchers' consideration for utilizing these materials to advance concrete blends. It is additionally of paramount significance to compare the impact on the mechanical properties of the Compressive Strength of concrete (CS). This is often because physical properties are utilized to assign the different properties of concrete, and the concrete situation is fundamentally based on CS [11], [12].

Admixtures utilizing inhomogeneous concrete of pozzolan influence the features of concrete by changing the cement base blend within the concrete [13]–[15]. Due to the little measure of silica, smolder can handle the double part of the filler and pozzolan in the concrete blend [16]. Concrete's short-term (28-day) compressive resistance will be enhanced despite an upgrade within the extent of micro-silica in concrete, which diminishes the workability of concrete [17]. The effective extent of silica-fume that has the most elevated compressive persistence has not continuously been accurately known. Analysts display a multi-ratio micro-silica supplant to attain the most extreme concrete CS [18], [19]. Since the estimation of particles is little compared to cement, the response of silica vapor appears like that of pozzolan, which enhances the concrete properties [20]–[24]. The utilization of micro-silica for fly ash next to the super-plasticizer can decrease porosity and lift the CS [25].

With a structure similar to Portland cement in shape and size, the fly ash component helps to reduce the amount of water in concrete production. Mixing optimally, fly ash and super-plasticizers improve the mechanical properties of concrete, mainly its compressive strength. Additionally, additives such as fly ash significantly impact strength, usability, concrete cost, and moisture penetration. Generally, fly ash is used to replace sticky substances. On the other hand, the use of fly ash in concrete mixtures positively affects the environment by reducing the risk of contamination [26]–[28]. The amount of fly ash replacement is about 20-50% of the total adhesive strength of concrete, and when the initial strength of concrete is the main factor, the amount of fly ash can increase up to 60% [29], [30].

Clever strategies like machine learning have had broad usage within the academic research fields. Specialists utilize these arrangements to gauge particular properties [31]–[33]. The presence of UHPC needs to encourage progress in artificial intelligence (AI) usage to decide the behavior of concrete beneath loads. Analysts in numerous examinations have effectively executed different strategies to recreate UHPC execution [34]–[36]. Even though these strategies demand information sets to construct vigorous models, the precision of outcomes relies on the species captured through the exploratory exertion or information sets acquired from authentic experiments. Research worked on the programming of gene expression calculation to assess the CS of concrete, including sugarcane ash remains [37]. In any case, model precision was calculated by comparing experimental quality estimations with model outputs. Another study created a model utilizing genetic programming to assess the compressive resistance of cement composed of micro-silica and nano-silica [38]. One article proposed a model that used an artificial neural network and optimized the model using a grey wolf optimization to predict the CS of micro-silica containing concrete and reduce the model's sophisticated, time, and energy supply [39].

By utilizing appropriate models, it is possible to obtain favorable results through the identification of optimal input combinations. Such an approach not only enables the realization of meaningful outcomes but also facilitates significant savings in terms of both time and financial resources. Empirical and statistical models, such as linear and nonlinear regression, have been extensively utilized in various fields of research [40], [41]. Nevertheless, the development of such models necessitates labor-intensive experimental undertakings and may generate imprecise outcomes in instances where the interdependencies between specific material attributes and the varying compositions and curing circumstances of the mixture are multifarious. Machine learning (ML) can be characterized as a subcategory of AI wherein an entity is capable of acquiring knowledge autonomously via algorithms [42]. This approach to learning involves leveraging datasets and past experiences to enhance overall performance, thereby enabling the entity to continually improve and refine its outputs. With minimal human involvement, machine learning algorithms exhibit the ability to learn autonomously and enhance their performance gradually over time [43]. ML has gained widespread adoption in the field of engineering as a versatile tool for the resolution of a range of issues. Examples include outage prediction, angular velocity estimation, component failure prognostics, and fatigue life prediction. The utilization of AI and ML has

been a prevalent approach in addressing obstacles encountered in diverse areas of structural engineering within the realm of civil engineering. The utilization of machine learning (ML) applications extends to the development of structural design and performance assessment, refinement of finite element modeling of structures, as well as enhancement of prediction and evaluation of concrete properties [44]–[46].

The aim of this study is used the machine learning method include Support Vector Regression (SVR) to predict the CS of UHPC output based on the experimental dataset. In addition, two meta-heuristic algorithms for optimizing have been used to solve the complex problem more accurately by determining key variables embedded in SVR containing Marine Predator Algorithm (MPA) and Grasshopper Optimization Algorithm (GOA). Moreover, several indices such as MAE, R2, RMSE, OBJ, and VAF were used to assess the process of modeling. Therefore, the SVR-GOA and SVR-MPA frameworks aim to evaluate the concrete persistence samples for training models developed using sample data from a mixture of UHPC and CS target values.

## 2. Materials and Methodology

To evaluate the compressive strength of UHPC, the evaluation of the model developed in this study is defined as one of the main objectives. Indeed, robust SVR models attempt to simulate CS values, which can help optimizers improve the quality of model results. Simultaneously, data sets must be processed, which is crucial for achieving that objective. Utilizing the GOA and MPA algorithms, the SVR finds the best solution for calculating the variables designated into the SVR, allowing the SVR-GOA and SVR-MPA to estimate CS close to the target measure. Therefore, providing a core data set for a feeding model that needs accurate measurements is necessary. With this regard, CS data sets for UHPC were collected from various experimental studies involving the same components [2], [52]–[54], [56]–[63]. In this regard, Fig. 1 has shown the ingredients dataset used to define and train the models plus the histograms of data frequency and normal distribution curve.

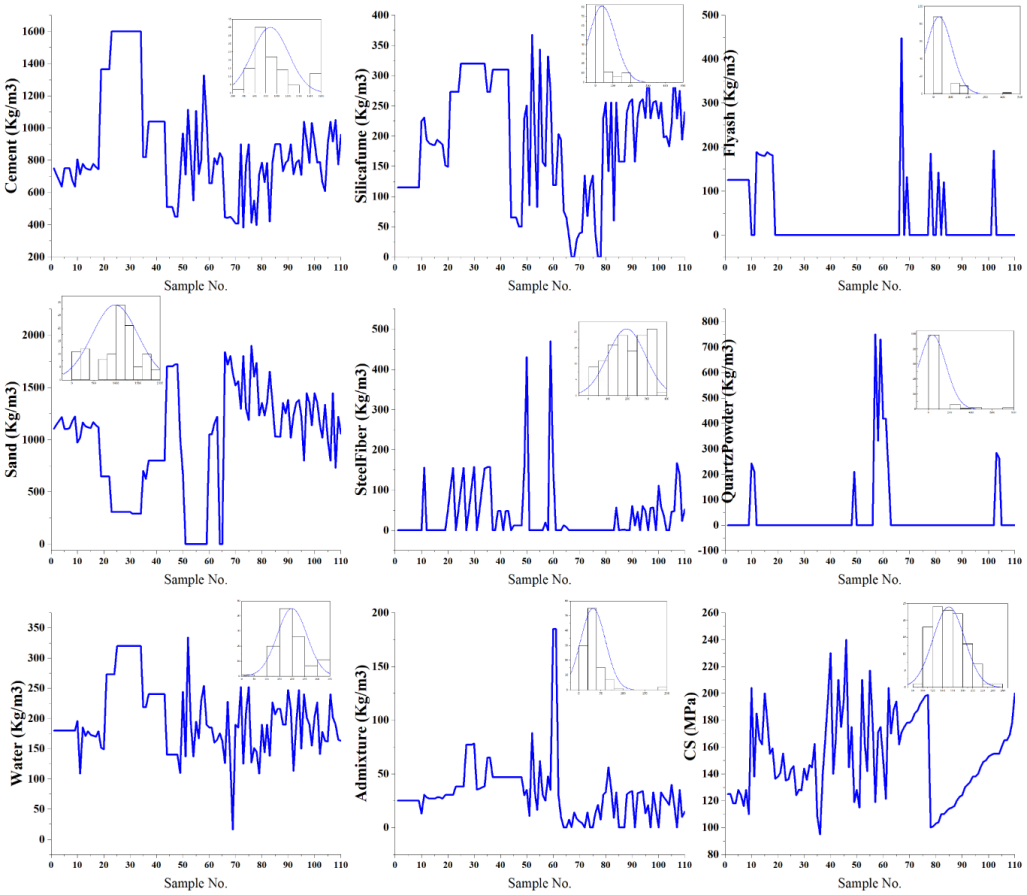


**Fig1**. The dataset used to define and train the models

Data gathered from 110 UHPC samples in the experiment are brought in briefly in Table 1. However, the information on components in the different magnitudes of UHPC samples may result in various CS in each sample.

UHPC Resistance modeling is performed by the mathematic strategies introduced in the following sections. Notably, all data are used for modeling in two phases: calibration (training) and validation (testing). 70 percent of data are considered for training and 30 percent for the testing stage.

**Table 1.** Input and target data for predictive models

| Component | Unit | Code | Statistical measurements | | | | |
|---|---|---|---|---|---|---|---|
| | | | Min | Max | Mean | Median | St. dev |
| Cement | (Kg/m3) | CE | 383 | 1600 | 879.7 | 786 | 329.8 |
| Fly ash | (Kg/m3) | FA | 120 | 448 | 33 | 120 | 72.7 |
| Sand | (Kg/m3) | SA | 292 | 1898 | 980 | 1107 | 513.8 |
| Steel fiber | (Kg/m3) | SF | 2 | 470 | 39 | 8 | 74.8 |
| Quartz powder | (Kg/m3) | QP | 203.3 | 750 | 36.9 | 211 | 125.9 |
| Compressive strength | (MPa) | CS | 95 | 240 | 152.2 | 147.9 | 31.5 |
| Admixture | (Kg/m3) | AD | 4 | 185 | 31.9 | 30.1 | 28.2 |
| Silica fume | (Kg/m3) | SI | 30 | 367.95 | 192 | 196 | 94.6 |
| Water | (Kg/m3) | WA | 109 | 334.5 | 197.1 | 185.3 | 54.3 |

### *2.1.Marine Predator Algorithm (MPA)*

The Marine Predators Algorithm (MPA) is the novel natural metaheuristic algorithm presented by Faramarzi *et al.* [64]. In the natural interaction among marine predators and prey, the predators employ a widely accepted foraging strategy named Brown and Levy random migration, inspired by the MPA. If the focus of prey in the hunting ground is high, the predator uses the Brown method, and if the prey is small, the Levy method is used. The Levy movement includes the shortened steps obeyed by jumps enhancing the process of exploration. However, the Brownian movement contains steps fixed in the same job for optimizing the exploitation process. Whereas matters of the environment such as fish aggregating devices (FADs) and eddy formation impacts are among the items that alter the predators' behavior. Fig. (2) shows the schematic view of the MPA mechanism [65]. The mathematical formulation of the MPA algorithm is as follows.

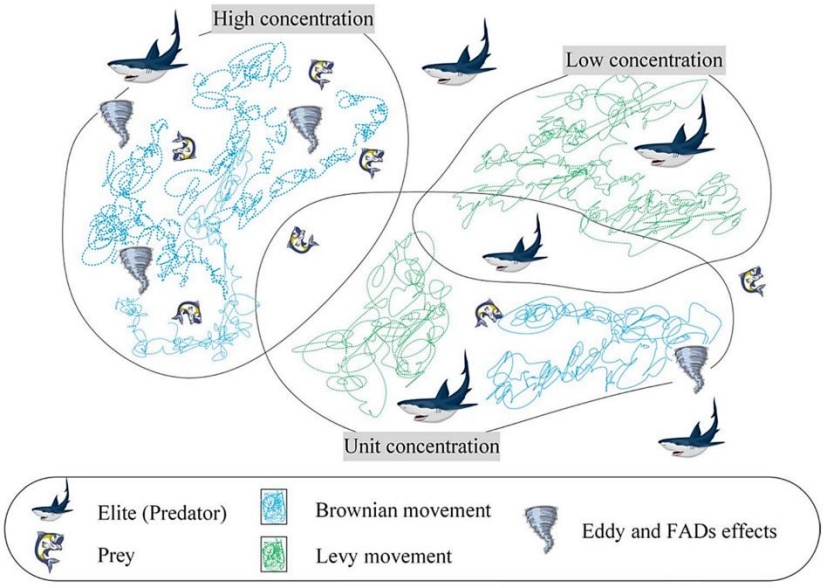


**Fig 2**. The biological interaction of marine predators and prey

The main stages of the MPA solution are explained as follows [51]:

The preys move with the Brownian motion, upgrading the matrices of Prey in Eq (1) and Eq (2):

$$\overrightarrow{step_J} = \overrightarrow{R_L} \otimes [\overrightarrow{elite_J} - (\overrightarrow{R_L} \otimes \overrightarrow{prey_J})] \quad (1)$$

$$\overrightarrow{prey_J} = \overrightarrow{prey_J} + (P.\vec{R} \otimes \overrightarrow{step_J}) \quad (2)$$

Wherein $R_L$ denotes a vector including accidental numbers based on the levy's movement. While the other half of the population is upgraded in Eq (3):

$$\overrightarrow{step_J} = \overrightarrow{R_B} \otimes ((\overrightarrow{R_B} \otimes \overrightarrow{elite_J}) - \overrightarrow{prey_J}) \quad (3)$$

$$\overrightarrow{prey_J} = \overrightarrow{elite_J} + (P.cf \otimes \overrightarrow{step_J}) \quad (4)$$

In which the matrix elite is assumed to multiply by $cf$. Eq. (5) defines the $cf$.

$$cf = [1 - (iter/max \times iter)]^{(2.iter/max \times iter)} \quad (5)$$

The predators move using Levy movement, and the matrix of prey is upgraded Eq. (6) and (7):

$$\overrightarrow{step_J} = \overrightarrow{R_L} \otimes ((\overrightarrow{R_L} \otimes \overrightarrow{elite_J}) - \overrightarrow{prey_J}) \quad (6)$$

$$\overrightarrow{prey_J} = \overrightarrow{elite_J} + (P.cf \otimes \overrightarrow{step_J}) \quad (7)$$

After each iteration, the matrix elite is upgraded with the best answers, and the final one will be introduced after the last iteration.

### 2.2. *Grasshopper optimization algorithm (GOA)*

Grasshopper optimization algorithm (GOA) as the swarm basis method simulates the behavior of the insect type of grasshopper in achieving the best answer [66]. Grasshoppers show the behavior of a swarm basis to move along the distance with two features of sudden movement and a long way. The mathematical behavior of grasshoppers is defined in Eq (8).

$$x_i = S_i + G_i + A_i \quad (8)$$

Wherein, $x_i$ shows the location of grasshopper $i$ and $S_i$ denotes the hereditary interaction of grasshoppers.

$$S_i = \sum_{\substack{j=1 \\ i \neq j}}^{N} s(d_{ij})\hat{d}_{ij} \ , \qquad d_{ij} = |x_i - x_j| \quad (9)$$

$$, \ \hat{d}_{ij} = \frac{x_i - x_j}{d_{ij}}$$

The parameter of $d_{ij}$ denotes the area among the grasshoppers of $i$ and $j$; $\hat{d}_{ij}$ is the unit vector between the grasshoppers $i$ and $j$; Also, $s$ represents the power of the group force.

$$s(x) = fe^{\frac{-x}{l}} - e^{-x} \quad (10)$$

Wherein, $f$ and $l$ denote the intensity of attraction and length, alternatively. The Nymph type grasshopper does not have wings, so the wind orientation is the crucial factor of insect motion.

$$A_i = u\hat{e}_w \ , \ G_i = -g\hat{e}_g \quad (11)$$

In which the parameters of $G_i$ and $A_i$ represent the gravity and advection of wind for the grasshopper$i$. The variable of $\hat{e}_g$ represents the unit vector that defines the direction of wind advection and the parameter of $\hat{e}_w$ shows the gravity orientation strength. Moreover, $u$ denotes the constant of wind drift, and $g$ mentions the gravity-fixed number. In this regard, Eq. (8) is regarded as Eq. (12):

$$X_j^d = c\left[\sum_{\substack{j=1 \\ i \neq j}}^{N} c\frac{ub_d - lb_d}{2} s(|x_i^d - x_j^d|)\frac{x_i - x_j}{d_{ij}}\right] + \hat{D}_d \quad (12)$$

Wherein the parameters of $ub_d$ and $lb_d$ are the up and low boundaries, $\hat{D}_d$ exhibits the dimension value of $d$, and the variable of $N$ denotes the population number. Moreover, $c$ shows the decrescent coefficient that is reduced with increasing the iterations to assist in balancing the operations of exploitation and exploration. This parameter enhances the exploitation as the iteration number is gone up.

$$c = c_{max} - Iter \times \frac{c_{max} - c_{min}}{M.Iter} \qquad \begin{cases} c_{max} = 1 \\ c_{min} = 0.0001 \end{cases} \quad (13)$$

### 2.3. *Support Vector Regression, SVR*

In this study, the SVR method (Support vector regression) method for classification regression issues was used [67]. SVR chooses an error region of ε to determine a regression model. It is noteworthy that categorization of the regression class can be performed to determine the specific bounds of the hyper plane. The SVR used in this study is regarded as a controlled method for determining the response to a regression process that develops the properties of the equation (14) [68].

$$min_{w,b} = \frac{1}{2}\|w\|^2 + C\sum_{i=1}^{m}(\xi_i + \xi_i^*),$$
$$const. \begin{Bmatrix} y_i - (w^T x_i + b) \leq \varepsilon + \xi_i \\ (w^T x_i + b) - y_i \leq \varepsilon + \xi_i^* \\ \xi_i, \xi_i^* \geq 0 \end{Bmatrix} \quad (14)$$

In Eq. (14), the variable of $y$ denotes the CS measurements; the boundary violation is determined by $\xi$ denotes; row regularizing is ascertained by $C$; the weight item is determined by $w$; $b$ also shows the SVR bias; Further, the $\varepsilon$ variable is the deviation magnitude of the boundary style of the hyper plane. Two terms written in Eq. (14) are analyzed in relations (15) and (16):

$$\frac{1}{2}\|w\|^2) \quad (15)$$

$$C\sum_{i=1}^{m}(\xi_i+\xi_i^*) \quad (16)$$

The term of $\frac{1}{2}\|w\|^2$ was brought in for increasing the area between the samples and boundary hyperplane to have the area from the samples to the boundaries. Moreover, the next term of relation (16) has worked as the adjuster tool. When developing operators to target the hyperplane boundary, collecting the values of $b$ and $w$ is required. A quadratic objective function is developed in current research, reaching the desired results to assign parameters ($C$, $\varepsilon$, and $sigma$) of SVR at the optimal levels [69]. Table 2 shows the abovementioned parameters calculated using optimization algorithms.

**Table 2**. The SVR key variables' values optimized

| | | SVR-MPA | SVR-AGO |
|---|---|---|---|
| **Training phase** | $C$ | 1.121 | 2.329 |
| | *EPSILON* | 1200 | 620 |
| | $sigma$ | 0.01 | 0.1 |
| **Testing Phase** | $C$ | 1.964 | 1.150 |
| | *EPSILON* | 1200 | 1200 |
| | $sigma$ | 1.100 | 1.288 |

In addition, Optimizers and Support Vector Regression (SVR) are two different concepts in machine learning. Optimizers are algorithms used to train a model by adjusting its parameters to minimize a loss function, while SVR is a type of regression algorithm used for predicting continuous values. However, it is possible to combine these two concepts to improve the performance of a machine learning model. One way to do this is to use the optimizer to tune the hyperparameters of the SVR model. Hyperparameters are parameters that are not learned during training but are set before training begins and affect the behavior of the model. For example, in SVR, the hyperparameters include the kernel function, the penalty parameter C, and the parameter epsilon. The kernel function determines the shape of the decision boundary used to make predictions, while the penalty parameter C and epsilon control the trade-off between the complexity of the model and its ability to fit the training data. By using an optimizer to tune these hyperparameters, it is possible to find the optimal values that improve the performance of the SVR model. This can be done by defining a loss function that measures the difference between the predicted values and the actual values and using an optimizer to minimize this loss function. Overall, the combination of optimizers and SVR can be a powerful tool for improving the performance of regression models and enabling researchers to develop more accurate and effective machine learning systems.

### *2.4. Evaluating criteria for models SVR-MPA and SVR-GOA*

In order to evaluate the models' effectiveness that wants to produce the compressive strength (CS) values of UHPC specimens for the calibration and validation phases, diverse indices are elaborated in Table 3

.

**Table 3**. Evaluation criteria to assess developed models

| Evaluation criteria | Nomenclature | Relations | Assessment |
|---|---|---|---|
| **Variance account factor** | *VAF* | $\left(1-\frac{var(t_n-y_n)}{var(t_n)}\right)*100$ (17) | Higher is desirable |
| **Mean absolute error** | *MAE* | $\frac{1}{N}\sum_{n=1}^{N}\lvert p_n-t_n\rvert$ (18) | Lower is desirable |
| **Root mean squared error** | *RMSE* | $\sqrt{\frac{1}{N}\sum_{n=1}^{N}(p_n-t_n)^2}$ (19) | Lower is desirable |

| | | | |
|---|---|---|---|
| **Pearson's correlation coefficient** | $R^2$ | $\left(\frac{\sum_{n=1}^{N}(t_n-\bar{t})(p_n-\bar{p})}{\sqrt{[\sum_{n=1}^{N}(t_n-\bar{p})^2][\sum_{n=1}^{N}(p_n-\bar{p})^2]}}\right)^2$ (20) | Higher is desirable |
| **Statistical parameters, including the various error indices** | $OBJ$ | $\left(\frac{n_{train}-n_{test}}{n_{train}+n_{test}}\right)\frac{RMSE_{train}+MAE_{test}}{R^2_{train}+1}+\left(\frac{2n_{train}}{n_{train}+n_{test}}\right)\frac{RMSE_{test}-MAE_{test}}{R^2_{test}+1}$ (21) | Lower is desirable [70] |

The metrics of the relations (17) - (21), the estimated compressive strength of samples UHPC is denoted via $p_N$; $t_n$ indicates CSs as measured target values; the $\bar{t}$ shows the averaged measurements of CS samples; $\bar{p}$ represents the averaged estimated CSs. Further, the ntrain and ntest indicate the number of samples collected for the calibration and validation phases, respectively.

## 3. Results and Discussion

The frameworks SVR-MPA and SVR-GOA were modeled, and the Compressive Strength (CS) of Ultra-High-Performance Concrete (UHPC) rates was generated based on the feeding data collected from the experimental research. Different ingredients were composed to create the samples considering 70 percent of the dataset for the training phase and the remaining for the validation (testing) phase. Five indices (as elaborated in Table 3) examined the outcomes with the target values to assess the proposed models' performance. The present study employs a methodology for the integration of the radial basis function (RBF) model with optimization techniques. This methodology leverages optimization techniques to ascertain the number of neurons and spread rate in the RBF network. The network structure parameters, exclusive of the activation function, were deemed optimization variables, with the radial basis function (RBF) serving as the cost function. In each iteration of the optimization process, the optimizers ascertained the variables, which were subsequently supplied as input to the cost function. The Root Mean Square Error (RMSE) was utilized to assess the cost rate in comparison with other cost rates and determine the minimum RMSE across a spectrum of iterations. The optimal configuration of the RBF network was determined by identifying the values of the variables that correspond to the minimum RMSE. To promote equitable comparison between the two hybrid models, a consistent number of iterations was employed along with an identical domain of variables. Consequently, Table 4 indicates the various metrics assessing the resultants of CS that are generated from the proposed models. Supposedly, the SVR-MPA was rated by the $R^2$ index in two phases, and in the training phase, it was calculated 90% which is 0.33% higher than SVR-GOA. Moreover, the $R^2$ of SVR-MPA was obtained at 95% for the testing phase, which is 3.04% higher than SVR-GOA.

**Table 4**. The CS assessing using various metrics

| | | | **SVR**-MPA | **SVR-GOA** | **Average** |
|---|---|---|---|---|---|
| **Criteria used** | Training step | $R^2$ | 0.901 | 0.898 | 0.899 |
| | | RMSE | 9.988 | 10.173 | 10.08 |
| | | MAE | 3.885 | 4.845 | 4.365 |
| | | VAF | 91.159 | 91.643 | 91.401 |
| | Testing step | $R^2$ | 0.946 | 0.918 | 0.932 |
| | | RMSE | 7.91 | 9.53 | 8.72 |
| | | MAE | 3.564 | 4.1 | 3.832 |
| | | VAF | 95.377 | 93.137 | 94.257 |
| | | OBJ | 6.458 | 7.43 | 6.944 |

The error indicator of RMSE also assessed the models that the MAP optimizer could get the error of 9.988 MPa in the validation stage, and the GOA algorithm achieved the 10.173 MPa, with a difference of 1.86%. The index of MAE also ranked the SVR-MPA and SVR-GOA in the training phase, at 3.885 MPa and 4.845 MPa, with a difference of 24.72%. For the VAF index, the MPA method could rate the relevant model at the level of 95.38, with a 2.41% highness

compared to SVR-GOA. The comprehensive assessment done by the OBJ index included all of the mentioned correlation and error indices (except for VAF). With this respect, in the validation phase, SVR-GOA was examined with this indicator at the rate of 7.42, which is 15.06% higher than SVR-MPA, with a value of 4.46.

Focusing on error distribution will help us better understand the modeling process for either of the frameworks. Regarding this matter, Fig. 2 shows the capability of each model to have errors concentrated around the zero rates. As shown in Fig. 3, the error histograms of SVR-MPA exhibit its appropriate distribution to make such tall bars around the zero point. Therefore, the normal distribution curve is formed as narrower-shaped rather than SVR-GOA's. While the histogram of this model's error is distributed non-uniformly, it has created the flattened curve of error normal distribution.

Considering the modeled results of CS for both models, Fig. 4 draws the observed rates against the estimated ones over the plots, including the best-fit line and the bisector of y=x. The SVR-MPA (a) could model the compressive strength values of samples close to SVR-GOA as the slope of the best-fit line has similar values of 0.85 and 0.84 for (a) and (b). However, the MPA appears to show better performance, leading to a more suitable distribution of CS points than GOA with exceeding points around the bisector line. However, the performance of each model is deserved to have an acceptable simulation quality.

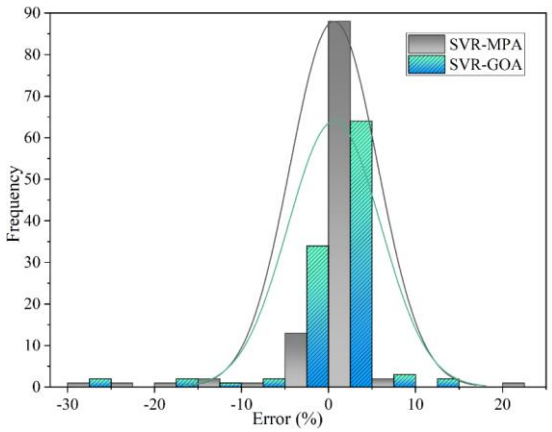


**Fig3**. The error normal distribution curve and error histograms

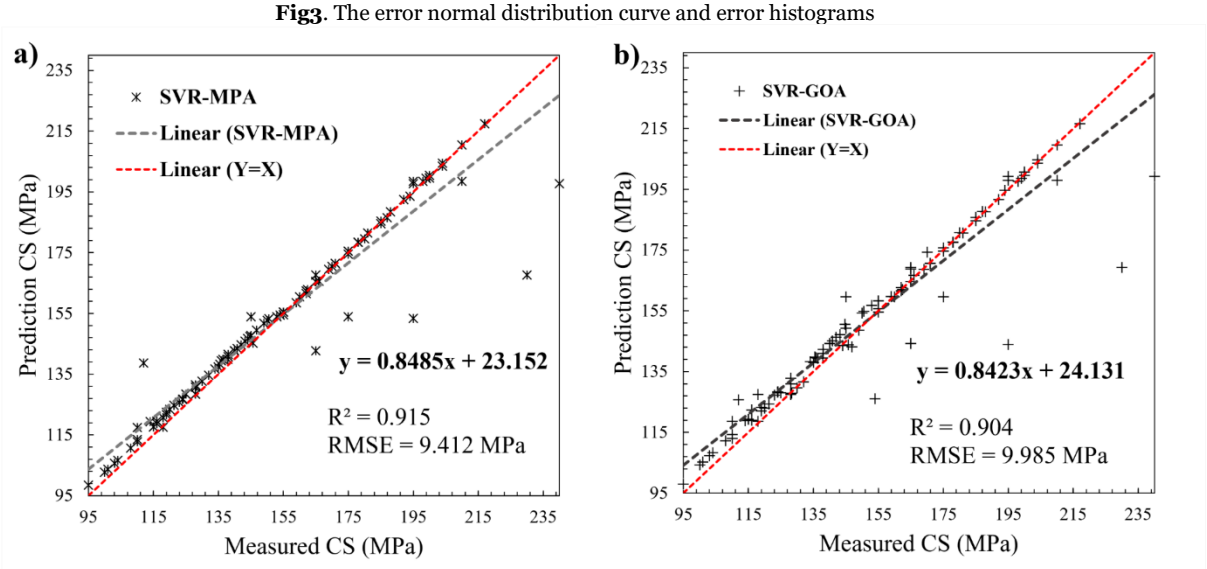


**Fig4**. Models' best-fit line for modeled and measured CSs for: a) SVR-MPA and b) SVR-GOA

Fig. 5 shows each sample's error computed in the modeling stage. In this regard, SVR-MPA (a) has modeled the CS based on ingredients entered to model with some cases in which there are overestimation and underestimation. This model has had five positions

exceeding the target values up to ±30% for the training phase. While for the validation stage, this range is reduced to -20% for the sample with several 100 with a -21.34% error as underestimated. On the other hand, for the SVR-GOA in the training phase, the errors are more than another model with error rates higher than ±10%. However, in the testing phase, the fluctuations of errors relative to the testing stage are reduced and the highest rate error is for the sample 100 with -26.23%, which is 23%, which is higher than the error calculated by the MPA optimizer.

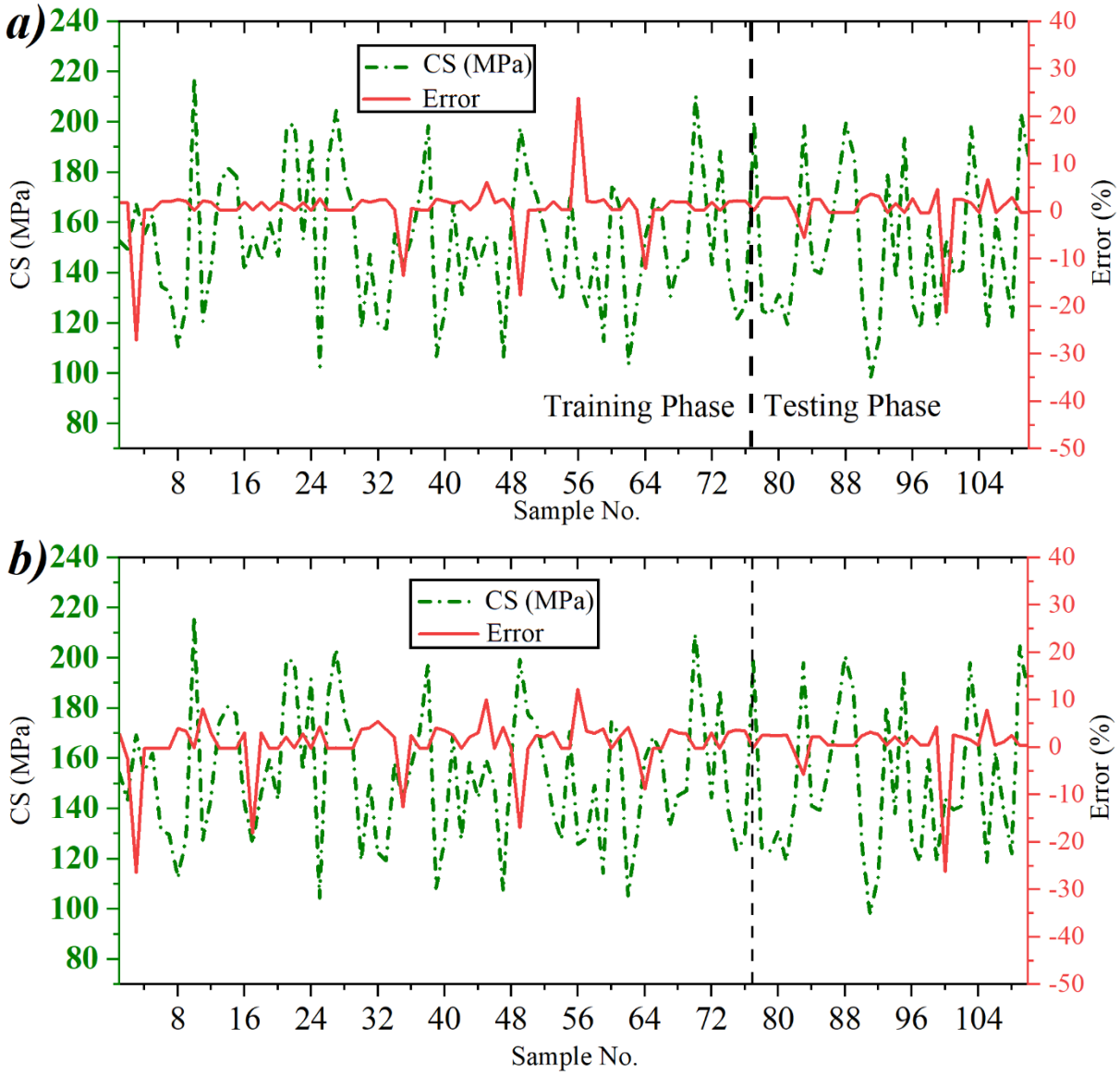


**Fig 5**. Error calculated for each sample with the CS modeled by: a) SVR-MPA and b) SVR-GOA

For comparing the difference of the CS calculated from both methods, Fig. 6 shows the discrepancy percentage for each of the samples. In fact, by dividing the CS modeled with SVR-GOA by SVR-MPA, this figure tries to draw a picture of the results of different calculation processes of two optimizers, MPA and GOA. Based on Fig. 6, there are many situations in which models have calculated CS differently from each other. In this regard, the sample of 11th with 5.62%, 17th with 18.38, 56th with 9.35%, and 99th with 6.21% difference are the remarkable values with higher differences in calculating the CS.

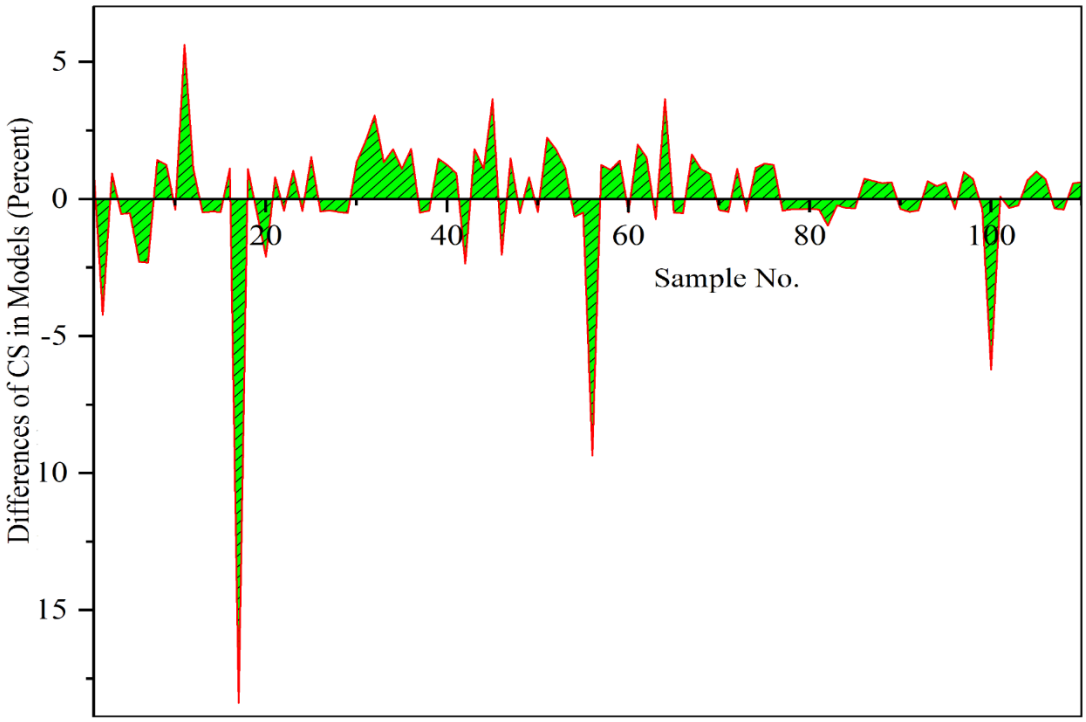


**Fig 6.** Differences of CS modeled by SVR-GOA/SVR-MPA

## 4. Conclusion

The concrete type called Ultra-High-Performance (UHPC) is developed for many projects that show excellent properties from the compressive behavior viewpoint and the tensile behavior and durability compared to typical concrete and high-performance concrete (HPC). This solution provides acceptable resistance against compressions up to 150 Mega Pascal (MPa) and excellent resistance in any harsh environment. By cutting the cement and micro-silica, the costs and emission of CO2 are reduced, further bringing the effective longer service life and properties compared to typical or high-strength concrete showing the high short-term cost and positive effects on the environment. This study attempts to simulate the UHPC samples' compressive strength, including environmentally friendly ingredients. For this reason, Support Vector Regression (SVR), a machine learning technique accompanied by the Marine Predator Algorithm (MPA) and Grasshopper Optimization Algorithm (GOA), was opted to model the Compressive Strength (CS) of UHPC. Eight items (introduced in Table 1) were mixed to create samples.

The SVR-MPA with R2 of 91.55% that modeled the CS rates more desirable than SVR-GOA could be better by being 1.25% more in terms of correlation factor this fact is clear in Fig. 4. For RMSE, SVR-GOA simulated the CSs with the error rate of 9.984 MPa while SVR-MPA conducted the job well with the RMSE of 6.08 percent lower than SVR-GOA. In the testing stage, either framework modeled the CS values in appropriate conditions that SVR-MPA reached the RMSE of 7.91 MPa, and for SVR-GOA, this was 9.53 MPa with a difference of 20.49%. The indicator of VAF also indicated the outcomes of both models close to one another. Based on VAF, The SVR-MPA outperformed appropriate than SVR-GOA with a difference of 0.53% in the training phase, while for validation, the difference was 2.41% percent in favor of the SVR-MPA with the values of 91.159 and 95.376 for training and testing phases, respectively. The comprehensive assessment done by the OBJ index included all of the mentioned correlation and error indices (except for VAF). With this respect, in the validation phase, SVR-GOA was examined with this indicator at the rate of 7.42, which is 15.06% higher than SVR-MPA, with a value of 4.46. Consequently, despite both frameworks modeling precisely at the acceptable range, the MPA optimizer could remove the errors well compared to the GOA algorithm, which is definitely seen in Fig. 3, which implies the concentration of errors adjacent to the zero point.

## REFERENCES

[1] B. A. Graybeal, "Material property characterization of ultra-high performance concrete," United States. Federal Highway Administration. Office of Infrastructure ..., 2006.
[2] B. A. Graybeal, "Compressive behavior of ultra-high-performance fiber-reinforced concrete," ACI Mater. J., vol. 104, no. 2, p. 146, 2007.

[3] P. Richard and M. Cheyrezy, “Composition of reactive powder concretes,” Cem. Concr. Res., vol. 25, no. 7, pp. 1501–1511, 1995.
[4] Y. L. Voo and S. J. Foster, “Characteristics of ultra-high performance ‘ductile’concrete and its impact on sustainable construction,” IES J. Part A Civ. Struct. Eng., vol. 3, no. 3, pp. 168–187, 2010.
[5] P. C. AITCIN, “Arts e scienza del calcestruzzo ad alte prestazioni,” L’Industria Ital. del Cem., vol. 68, no. 731, pp. 350–365, 1998.
[6] F. P. Torgal and S. Jalali, “Cement composites reinforced with vegetable fibres,” in Eco-efficient Construction and Building Materials, Springer, 2011, pp. 143–156.
[7] C. Shi, Z. Wu, J. Xiao, D. Wang, Z. Huang, and Z. Fang, “A review on ultra high performance concrete: Part I. Raw materials and mixture design,” Constr. Build. Mater., vol. 101, pp. 741–751, 2015.
[8] Z. Yunsheng, S. Wei, L. Sifeng, J. Chujie, and L. Jianzhong, “Preparation of C200 green reactive powder concrete and its static–dynamic behaviors,” Cem. Concr. Compos., vol. 30, no. 9, pp. 831–838, 2008.
[9] W. Zheng, B. Luo, and Y. Wang, “Compressive and tensile properties of reactive powder concrete with steel fibres at elevated temperatures,” Constr. Build. Mater., vol. 41, pp. 844–851, 2013.
[10] A. A. Pishro and X. Feng, “Experimental Study on Bond Stress between Ultra High Performance Concrete and Steel Reinforcement,” Civ. Eng. J., vol. 3, no. 12, pp. 1235–1246, 2018.
[11] Y. K. Cho, S. H. Jung, and Y. C. Choi, “Effects of chemical composition of fly ash on compressive strength of fly ash cement mortar,” Constr. Build. Mater., vol. 204, pp. 255–264, Apr. 2019, doi: 10.1016/j.conbuildmat.2019.01.208.
[12] M. Lezgy-Nazargah, S. A. Emamian, E. Aghasizadeh, and M. Khani, “Predicting the mechanical properties of ordinary concrete and nano-silica concrete using micromechanical methods,” Sādhanā, vol. 43, no. 12, p. 196, Dec. 2018, doi: 10.1007/s12046-018-0965-0.
[13] L. G. Li, J. Zhu, Z. H. Huang, A. K. H. Kwan, and L. J. Li, “Combined effects of micro-silica and nano-silica on durability of mortar,” Constr. Build. Mater., vol. 157, pp. 337–347, Dec. 2017, doi: 10.1016/j.conbuildmat.2017.09.105.
[14] H. Eskandari, A. M. Nic, and A. Ghanei, “Effect of Air Entraining Admixture on Corrosion of Reinforced Concrete,” Procedia Eng., vol. 150, pp. 2178–2184, 2016, doi: 10.1016/j.proeng.2016.07.261.
[15] A. Madadi, H. Eskandari-Naddaf, and M. Gharouni-Nik, “Lightweight Ferrocement Matrix Compressive Behavior: Experiments Versus Finite Element Analysis,” Arab. J. Sci. Eng., vol. 42, no. 9, pp. 4001–4013, Sep. 2017, doi: 10.1007/s13369-017-2557-4.
[16] B. B. Sabir, “Mechanical properties and frost resistance of silica fume concrete,” Cem. Concr. Compos., vol. 19, no. 4, pp. 285–294, 1997.
[17] M. Mazloom, A. A. Ramezanianpour, and J. J. Brooks, “Effect of silica fume on mechanical properties of high-strength concrete,” Cem. Concr. Compos., vol. 26, no. 4, pp. 347–357, 2004.
[18][ S. Bhanja and B. Sengupta, “Influence of silica fume on the tensile strength of concrete,” Cem. Concr. Res., vol. 35, no. 4, pp. 743–747, 2005.
[19] M. Y. Mansour, M. Dicleli, J. Y. Lee, and J. Zhang, “Predicting the shear strength of reinforced concrete beams using artificial neural networks,” Eng. Struct., vol. 26, no. 6, pp. 781–799, May 2004, doi: 10.1016/j.engstruct.2004.01.011.
[20] Z. Bajja, W. Dridi, A. Darquennes, R. Bennacer, P. Le Bescop, and M. Rahim, “Influence of slurried silica fume on microstructure and tritiated water diffusivity of cement pastes,” Constr. Build. Mater., vol. 132, pp. 85–93, Feb. 2017, doi: 10.1016/j.conbuildmat.2016.11.097.
[21] M. Rostami and K. Behfarnia, “The effect of silica fume on durability of alkali activated slag concrete,” Constr. Build. Mater., vol. 134, pp. 262–268, Mar. 2017, doi: 10.1016/j.conbuildmat.2016.12.072.
[22] H. Li, H. Xiao, J. Yuan, and J. Ou, “Microstructure of cement mortar with nano-particles,” Compos. Part B Eng., vol. 35, no. 2, pp. 185–189, Mar. 2004, doi: 10.1016/S1359-8368(03)00052-0.
[23] A. K. Mukhopadhyay, “Next-generation nano-based concrete construction products: a review,” Nanotechnol. Civ. Infrastruct., pp. 207–223, 2011.
[24] L. G. Li, J. Y. Zheng, J. Zhu, and A. K. H. Kwan, “Combined usage of micro-silica and nano-silica in concrete: SP demand, cementing efficiencies and synergistic effect,” Constr. Build. Mater., vol. 168, pp. 622–632, Apr. 2018, doi: 10.1016/j.conbuildmat.2018.02.181.
[25] M. Jalal, A. Pouladkhan, O. F. Harandi, and D. Jafari, “RETRACTED: Comparative study on effects of Class F fly ash, nano silica and silica fume on properties of high performance self compacting concrete,” Constr. Build. Mater., vol. 94, pp. 90–104, Sep. 2015, doi: 10.1016/j.conbuildmat.2015.07.001.
[26] J.-S. Chou and A.-D. Pham, “Smart Artificial Firefly Colony Algorithm-Based Support Vector Regression for Enhanced Forecasting in Civil Engineering,” Comput. Civ. Infrastruct. Eng., vol. 30, no. 9, pp. 715–732, Sep. 2015, doi: 10.1111/mice.12121.
[27] M. H. Rafiei, W. H. Khushefati, R. Demirboga, and H. Adeli, “Supervised deep restricted Boltzmann machine for estimation of concrete,” ACI Mater. J., vol. 114, no. 2, p. 237, 2017.
[28] M. Castelli, L. Trujillo, I. Goncalves, and A. Popovic, “An evolutionary system for the prediction of high performance concrete strength based on semantic genetic programming,” Comput. Concr., vol. 19, no. 6, pp. 651–658, 2017.
[29] L. Lam, Y. . Wong, and C. . Poon, “Effect of Fly Ash and Silica Fume on Compressive and Fracture Behaviors of Concrete,” Cem. Concr. Res., vol. 28, no. 2, pp. 271–283, Feb. 1998, doi: 10.1016/S0008-8846(97)00269-X.
[30] K. G. Babu and G. S. N. Rao, “Early strength behaviour of fly ash concretes,” Cem. Concr. Res., vol. 24, no. 2, pp. 277–284, 1994.

[31] Ł. Sadowski, M. Nikoo, and M. Nikoo, "Concrete compressive strength prediction using the imperialist competitive algorithm," Comput. Concr. An Int. J., vol. 22, no. 4, pp. 355–363, 2018.
[32] S. Czarnecki, M. Shariq, M. Nikoo, and Ł. Sadowski, "An intelligent model for the prediction of the compressive strength of cementitious composites with ground granulated blast furnace slag based on ultrasonic pulse velocity measurements," Measurement, vol. 172, p. 108951, Feb. 2021, doi: 10.1016/j.measurement.2020.108951.
[33] Ł. Sadowski, M. Piechówka-Mielnik, T. Widziszowski, A. Gardynik, and S. Mackiewicz, "Hybrid ultrasonic-neural prediction of the compressive strength of environmentally friendly concrete screeds with high volume of waste quartz mineral dust," J. Clean. Prod., vol. 212, pp. 727–740, 2019.
[34] C. T. G. Awodiji, D. O. Onwuka, C. Okere, and O. Ibearugbulem, "Anticipating the compressive strength of hydrated lime cement concrete using artificial neural network model," Civ. Eng. J., vol. 4, no. 12, pp. 3005–3018, 2018.
[35] J. Kasperkiewicz, J. Racz, and A. Dubrawski, "HPC strength prediction using artificial neural network," J. Comput. Civ. Eng., vol. 9, no. 4, pp. 279–284, 1995.
[36] E. Ghafari, M. Bandarabadi, H. Costa, and E. Júlio, "Design of UHPC using artificial neural networks," in Brittle Matrix Composites 10, Elsevier, 2012, pp. 61–69.
[37] M. F. Javed et al., "Applications of gene expression programming and regression techniques for estimating compressive strength of bagasse ash based concrete," Crystals, vol. 10, no. 9, p. 737, 2020.
[38] S. A. Emamian and H. Eskandari-Naddaf, "Genetic programming based formulation for compressive and flexural strength of cement mortar containing nano and micro silica after freeze and thaw cycles," Constr. Build. Mater., vol. 241, p. 118027, Apr. 2020, doi: 10.1016/j.conbuildmat.2020.118027.
[39] A. Behnood and E. M. Golafshani, "Predicting the compressive strength of silica fume concrete using hybrid artificial neural network with multi-objective grey wolves," J. Clean. Prod., vol. 202, pp. 54–64, 2018.
[40] R. S. Benemaran and M. Esmaeili-Falak, "Optimization of cost and mechanical properties of concrete with admixtures using MARS and PSO," Comput. Concr., vol. 26, no. 4, pp. 309–316, 2020, doi: 10.12989/cac.2020.26.4.309.
[41] R. Sarkhani Benemaran, M. Esmaeili-Falak, and A. Javadi, "Predicting resilient modulus of flexible pavement foundation using extreme gradient boosting based optimised models," Int. J. Pavement Eng., pp. 1–20, 2022.
[42] L. Huang, W. Jiang, Y. Wang, Y. Zhu, and M. Afzal, "Prediction of long-term compressive strength of concrete with admixtures using hybrid swarm-based algorithms," Smart Struct. Syst., vol. 29, no. 3, pp. 433–444, 2022.
[43] M. Esmaeili-Falak and R. S. Benemaran, "Ensemble deep learning-based models to predict the resilient modulus of modified base materials subjected to wet-dry cycles," Geomech. Eng., 2023.
[44] Z. Nurlan, "A novel hybrid radial basis function method for predicting the fresh and hardened properties of self-compacting concrete," Adv. Eng. Intell. Syst., vol. 1, no. 01, 2022.
[45] H. Cheng, S. Kitchen, and G. Daniels, "Novel hybrid radial based neural network model on predicting the compressive strength of long-term HPC concrete," Adv. Eng. Intell. Syst., vol. 1, no. 02, 2022.
[46] R. S. Benemaran, "Application of extreme gradient boosting method for evaluating the properties of episodic failure of borehole breakout," Geoenergy Sci. Eng., p. 211837, 2023.
[47] J. Luo, H. Chen, Y. Xu, H. Huang, and X. Zhao, "An improved grasshopper optimization algorithm with application to financial stress prediction," Appl. Math. Model., vol. 64, pp. 654–668, 2018.
[48] X. Zhang, Q. Miao, H. Zhang, and L. Wang, "A parameter-adaptive VMD method based on grasshopper optimization algorithm to analyze vibration signals from rotating machinery," Mech. Syst. Signal Process., vol. 108, pp. 58–
[49] A. H. Yakout, H. Kotb, H. M. Hasanien, and K. M. Aboras, "Optimal fuzzy PIDF load frequency controller for hybrid microgrid system using marine predator algorithm," IEEE Access, vol. 9, pp. 54220–54232, 2021.
[50] N. H. Khan, R. Jamal, M. Ebeed, S. Kamel, H. Zeinoddini-Meymand, and H. M. Zawbaa, "Adopting Scenario-Based approach to solve optimal reactive power Dispatch problem with integration of wind and solar energy using improved Marine predator algorithm," Ain Shams Eng. J., vol. 13, no. 5, p. 101726, 2022.
[51] A. H. Yakout, M. A. Attia, and H. Kotb, "Marine predator algorithm based cascaded PIDA load frequency controller for electric power systems with wave energy conversion systems," Alexandria Eng. J., vol. 60, no. 4, pp. 4213–4222, 2021.
[52] M. Hassan and K. Wille, "Experimental impact analysis on ultra-high performance concrete (UHPC) for achieving stress equilibrium (SE) and constant strain rate (CSR) in Split Hopkinson pressure bar (SHPB) using pulse shaping technique," Constr. Build. Mater., vol. 144, pp. 747–757, Jul. 2017, doi: 10.1016/j.conbuildmat.2017.03.185.
[53] H.-O. Jang, H.-S. Lee, K. Cho, and J. Kim, "Experimental study on shear performance of plain construction joints integrated with ultra-high performance concrete (UHPC)," Constr. Build. Mater., vol. 152, pp. 16–23, Oct. 2017, doi: 10.1016/j.conbuildmat.2017.06.156.
[54] K. Wille and C. Boisvert-Cotulio, "Material efficiency in the design of ultra-high performance concrete," Constr. Build. Mater., vol. 86, pp. 33–43, Jul. 2015, doi: 10.1016/j.conbuildmat.2015.03.087.
[55] K.-Q. Yu, J.-T. Yu, J.-G. Dai, Z.-D. Lu, and S. P. Shah, "Development of ultra-high performance engineered cementitious composites using polyethylene (PE) fibers," Constr. Build. Mater., vol. 158, pp. 217–227, 2018.
[56] K. Habel, M. Viviani, E. Denarié, and E. Brühwiler, "Development of the mechanical properties of an ultra-high

performance fiber reinforced concrete (UHPFRC)," Cem. Concr. Res., vol. 36, no. 7, pp. 1362–1370, 2006.
[57] M. Ghrici, S. Kenai, and M. Said-Mansour, "Mechanical properties and durability of mortar and concrete containing natural pozzolana and limestone blended cements," Cem. Concr. Compos., vol. 29, no. 7, pp. 542–549, Aug. 2007, doi: 10.1016/j.cemconcomp.2007.04.009.
[58] A. M. T. Hassan, S. W. Jones, and G. H. Mahmud, "Experimental test methods to determine the uniaxial tensile and compressive behaviour of ultra high performance fibre reinforced concrete (UHPFRC)," Constr. Build. Mater., vol. 37, pp. 874–882, Dec. 2012, doi: 10.1016/j.conbuildmat.2012.04.030.
[59] M. Shafieifar, M. Farzad, and A. Azizinamini, "Experimental and numerical study on mechanical properties of Ultra High Performance Concrete (UHPC)," Constr. Build. Mater., vol. 156, pp. 402–411, Dec. 2017, doi: 10.1016/j.conbuildmat.2017.08.170.
[60] A. Alsalman, C. N. Dang, G. S. Prinz, and W. M. Hale, "Evaluation of modulus of elasticity of ultra-high performance concrete," Constr. Build. Mater., vol. 153, pp. 918–928, Oct. 2017, doi: 10.1016/j.conbuildmat.2017.07.158.
[61] R. Zhong, K. Wille, and R. Viegas, "Material efficiency in the design of UHPC paste from a life cycle point of view," Constr. Build. Mater., vol. 160, pp. 505–513, 2018.
[62] M. Alkaysi and S. El-Tawil, "Factors affecting bond development between Ultra High Performance Concrete (UHPC) and steel bar reinforcement," Constr. Build. Mater., vol. 144, pp. 412–422, Jul. 2017, doi: 10.1016/j.conbuildmat.2017.03.091.
[63] M. G. Sohail et al., "Advancements in Concrete Mix Designs: High-Performance and Ultrahigh-Performance Concretes from 1970 to 2016," J. Mater. Civ. Eng., vol. 30, no. 3, p. 04017310, Mar. 2018, doi: 10.1061/(ASCE)MT.1943-5533.0002144.
[64] A. Faramarzi, M. Heidarinejad, S. Mirjalili, and A. H. Gandomi, "Marine Predators Algorithm: A nature-inspired metaheuristic," Expert Syst. Appl., vol. 152, p. 113377, 2020.
[65] M. Ramezani, D. Bahmanyar, and N. Razmjooy, "A new improved model of marine predator algorithm for optimization problems," Arab. J. Sci. Eng., vol. 46, no. 9, pp. 8803–8826, 2021.
[66] S. Saremi, S. Mirjalili, and A. Lewis, "Grasshopper optimisation algorithm: theory and application," Adv. Eng. Softw., vol. 105, pp. 30–47, 2017.
[67] L. Wang, Support vector machines: theory and applications, vol. 177. Springer Science & Business Media, 2005.
[68] V. Vapnik, The nature of statistical learning theory. Springer science & business media, 2013.
[69] A. Al-Fugara, M. Ahmadlou, A. R. Al-Shabeeb, S. AlAyyash, H. Al-Amoush, and R. Al-Adamat, "Spatial mapping of groundwater springs potentiality using grid search-based and genetic algorithm-based support vector regression," Geocarto Int., pp. 1–20, Jan. 2020, doi: 10.1080/10106049.2020.1716396.
[70] G. Pazouki, E. M. Golafshani, and A. Behnood, "Predicting the compressive strength of self-compacting concrete containing Class F fly ash using metaheuristic radial basis function neural network," Struct. Concr., vol. 23, no. 2, pp. 1191–1213, 2022.